A SHAPE MEMORY POLYMER ADHESIVE GRIPPER FOR PICK-AND-PLACE APPLICATIONS

BY

CHANGHEE SON

THESIS

Submitted in partial fulfillment of the requirements
for the degree of Master of Science in Mechanical Engineering
in the Graduate College of the
University of Illinois at Urbana-Champaign, 2019

Urbana, Illinois

Adviser:

Associate Professor Seok Kim

ABSTRACT

Over the past few years, shape memory polymers (SMPs) have been extensively studied in term of their remarkable reversible dry adhesive properties and related smart adhesive applications. However, these exceptional properties of SMPs have not been exploited for pick-and-place applications, which would otherwise advance the robotic manipulation. This work explores the use of SMPs to design an adhesive gripper which pick and place target solid objects relying on reversible dry adhesion of SMP. Compared with common finger or soft grippers, the SMP adhesive gripper interacts with a single surface of a target object for pick-and-place. Furthermore, it is easy and inexpensive to manufacture and applicable to various surfaces since it involves reversible dry adhesion. In this paper, associated physical mechanisms and temperature analyses are studied and conducted. Also, the study includes manufacturing of a dual SMP and a release tip which substantially enhances the adhesion strength and considerably minimizes the releasing force. Finally, the versatility and utility of the SMP adhesive gripper are demonstrated through pick-and-place experiments.

TABLE OF CONTENTS

CHAPTER 1: INTRODUCTION

The recent research on robotic grippers targets at developing pick-and-place devices, climbing robots or both. In particular, many researchers have been studying these robotic grippers since the demand of those devices has grown in various fields. For example, the aerospace industry requires gravity-independent grippers [1], the electronics industry needs pick-and-place manipulations via surface mounting technologies [2]. The manufacturing or logistics industry has also strong demand on heavy object lifting grippers or repetitive grippers that can lessen the burden of human workers [3-5]. The microelectromechanical systems (MEMS) industry also utilizes grippers for micro assembly [6].

Various mechanisms for robotic grippers have been introduced. For example, finger grippers are simple but effective grippers which can be optimized by choosing the number of fingers and the shape of their gripping motions with appropriate actuation methods [7-9]. Soft grippers are also promising since they resemble real human fingers [10]. Using microspine grippers can be a great choice to interact with rough surfaces such as rocks [1,11]. Magnetic grippers have a benefit of easy and fast pick-up and releasing [12]. Vacuum grippers are capable for heavy weight lifting such that it can also be used for climbing [13-14]. More recent gecko grippers, unlike vacuum grippers, do not need any atmosphere so that it can also be used in space [15-16]. Also, electroadhesion grippers based on the electrostatic force are beneficial for quick picking and placing since it is a electrically controlled actuator [17].

However, both finger and soft grippers have a common drawback that the target objects they are lifting have to have multiple surfaces with appropriate dimensions to be gripped. Magnetic grippers can pick and release only ferrous materials. Microspine grippers are not capable of working for smooth surface objects. Vacuum grippers would not work in vacuum nor for porous surface objects. Gecko grippers require directional shear forces and somewhat complicated manufacturing processes. Electroadhesion based gripper are not capable for high strength adhesion.

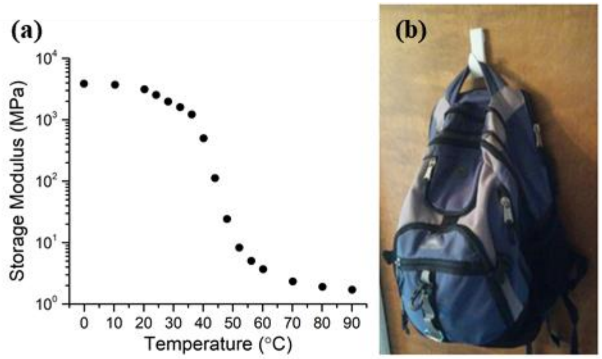

Figure 1 (a) The storage modulus of a shape memory polymer (SMP) as a function of temperature. (b) Application of the SMP as a reversible dry adhesive hook.

In this work, a shape memory polymer (SMP) is exploited to design an adhesive gripper due to its unique reversible dry adhesive abilities which eliminate or mitigate the challenges of other existing grippers. An SMP is a class of external-stimuli responsive polymer with the ability to memorize its 'permanent shape' which is recoverable from a deformed shape, i.e. 'temporary shape'. In particular, a thermoresponsive SMP undergoes a dramatic change in storage modulus across the glass transition temperature (T_g) between glassy and rubbery states, and generally shows a strong shape memory effect, i.e., ability to stably fix its temporary shape and fully recover its permanent shape [18-21]. As suggested elsewhere [22], the adhesion strength (F) of a reversible dry adhesive is inversely proportional to the square root of the adhesive system compliance (C) when material properties and true contact area (A) associated with the adhesive-adherend interface are fixed. Consequently, F is controlled by C in addition to A, which causes a contradictory condition that an adhesive material must be soft enough to make a conformal contact and increase A with an adherend but stiff enough to minimize C. An SMP is uniquely suited to satisfy this condition since its storage modulus can be changed dynamically (Fig. 1a), and therefore a conformal contact with large A can be formed in the rubbery state and be maintained in the glassy state where C is minimized because of the strong temporary shape fixing. By exploring these unique properties of an SMP, recently a consumer product-like prototype of a reversible adhesive hook was demonstrated as depicted in Fig. 1b [18].

CHAPTER 2: METHODS

2.1 Pick-and-Place Procedure

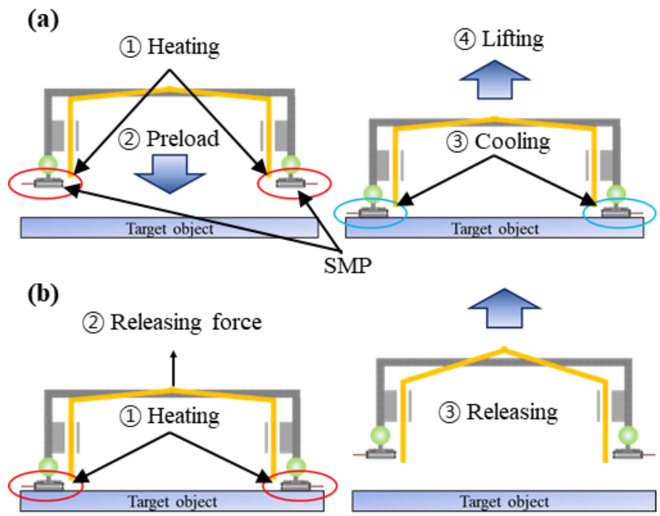

Figure 2 The target object is (a) picked up in sequential steps of SMP heating, preloading, SMP cooling and lifting. (b) The SMP is heated and release force is applied to peel the SMP and release the target object.

The steps of how the SMP adhesive gripper work is shown in Fig. 2. In the picking step, the SMP is heated up to the rubbery state. Then the preload is applied and the SMP is cooled down to the glassy state simultaneously. At this state, the gripper is attached to the target object and is ready to lift due to the strong dry adhesion of the SMP. In the placing step, similarly, the SMP is heated up to the rubbery state and thus to the weak adhesion state. After heating with the operator's manipulation, releasing force is applied to peel the SMP. As a result, the gripper is able to be separated from the target object.

2.2 Schematics

The computer-aided design model and the actual image of the SMP adhesive gripper which has three legs and feet are shown in Fig. 3. The body is built primarily with machined aluminum and 3D printed parts. The three feet are all connected to an 11.1 V, 1200 mAh Lithium

Polymer (LiPo) battery purchased from Kinexsis. Wires between feet and the external lead of the gripper are concealed inside aluminum frames. Three Peltier modules are under three feet and utilized for heating/cooling cycles. To control the Peltier modules by switching electrical polarity, i.e., the direction of current flow, 15 ampere maximum double-pole, double-throw (DPDT) switch with ‘center position off’ is used.

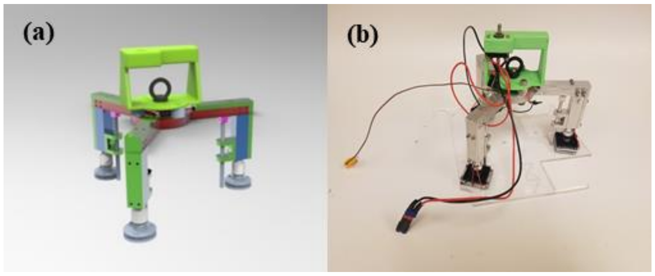

Figure 3 (a) The CAD drawing and (b) the optical image of an SMP adhesive gripper. The gripper has one battery input and one thermocouple output for heating/cooling cycles and measuring the temperature of the SMP.

2.3 Fabrication of SMP

The SMP that is used in this research was prepared based on the procedure developed elsewhere [18]. First, Poly(Bisphenol A-co-epichlorohydrin), glycidyl end-capped with a molecular weight of 1075 g/mol from Sigma-Aldrich, hereafter called E1075, and EPON 826 with a molecular weight of 362 g/mol from Momentive are preheated in a 110 °C oven. When E1075 is completely melted, E1075 and EPON 826 is thoroughly mixed to make the epoxy monomer. The curing agent Jeffamine D-230 poly(propylene glycol)bis(2-aminopropyl) ether with an average molecular weight of about 230 from Huntsman, hereafter called Jeffamine, is then included into the epoxy monomer and thoroughly mixed. Each chemical is mixed in a weight-based ratio of E1075:EPON 826:Jeffamine to be as 0.940:1.000:0.837 for the stiff SMP and 0.334:1.000:0.707 for the soft SMP. The resulting mixture is poured on a PTFE tape(Tapecase) which is adhered on a 3 x 2 inch glass slide and air bubbles inside the mixture are removed with a pipette. The curing takes place in a hot oven for 120 minutes at 80 °C. After the

SMP is fully cured, it is easily peeled off from the PTFE tape at a glassy state. For the single SMP, the peeled-off SMP is cut into a round shape of 25mm diameter using Fusion M2 laser cutter from Epilog Laser(Fig. 4(a)). For the dual SMP, the peeled-off SMP of the soft mixture ratio is cut into a 5mm width doughnut shape using the laser printer – 25 mm outer diameter and 15 mm inner diameter. The center hollow area is then filled up with the stiff SMP and then cured(Fig. 4(b)). The final SMP sample is then adhered to backing aluminum block using Loctite Instant Mix epoxy.

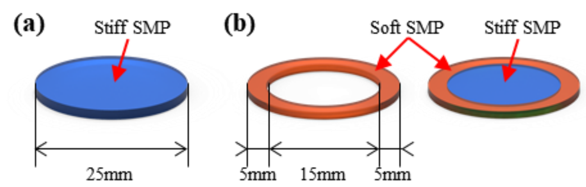

Figure 4 (a) Fabrication of the single SMP sample. The stiff SMP is cured and cut into 25mm diameter sized round shape using the laser cutter. (b) Fabrication of the dual SMP sample. The soft SMP is cured and then cut into a ring shape using the laser printer. Then, stiff SMP is cured inside the ring-shaped SMP.

For the fabrication of the SMP with release tip, the cured stiff SMP is cut into a round shape of 25mm diameter using the laser cutter. Then, a single drop of new uncured stiff SMP is placed on the cured SMP using a pipette. As shown in Fig. 5(b) the measured position from the center is 8.5 mm away, its radius is 5.08 mm and the maximum height is 0.64 mm.

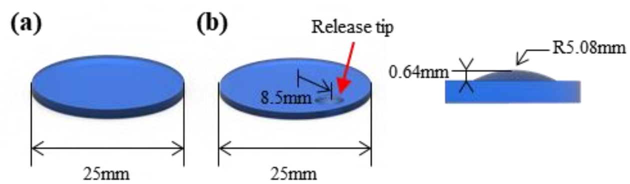

Figure 5 (a) Fabrication of the SMP without tip. The SMP is cured and cut into 25mm diameter sized round shape using the laser cutter. This sample is identical to the single SMP introduced previously. (b) Fabrication of SMP with release tip. SMP is cured and cut into a round shape. Then, SMP tip with the same ingredients is put on to the original SMP using the pipette and then cured.

2.4 Test Setup

The test setup for the maximum adhesion strength test and the peeling strength test is shown in Fig. 6. The glassy state SMP is fixed to the backing aluminum block and the block is connected to a bucket across the pulleys using fishing wires. The block has an embedded cartridge heater and a thermo couple which is connected to a temperature controller. The block is heated until the SMP turns into the rubbery state. Then the preload of 12.67 kg (2.50 atm) is given to achieve conformal contact between the SMP and the acrylic target plate while it is being cooled. After the SMP cools and turns back into the glassy state the maximum adhesion strength can be measured by slowly pumping water into the bucket. Otherwise, the SMP can be reheated until it becomes rubbery state again and measure the minimum peeling strength by slowly pumping water into the bucket. The maximum adhesion strength or the minimum peeling strength is recorded when the SMP detaches from the target plane as shown in Fig. 6(b).

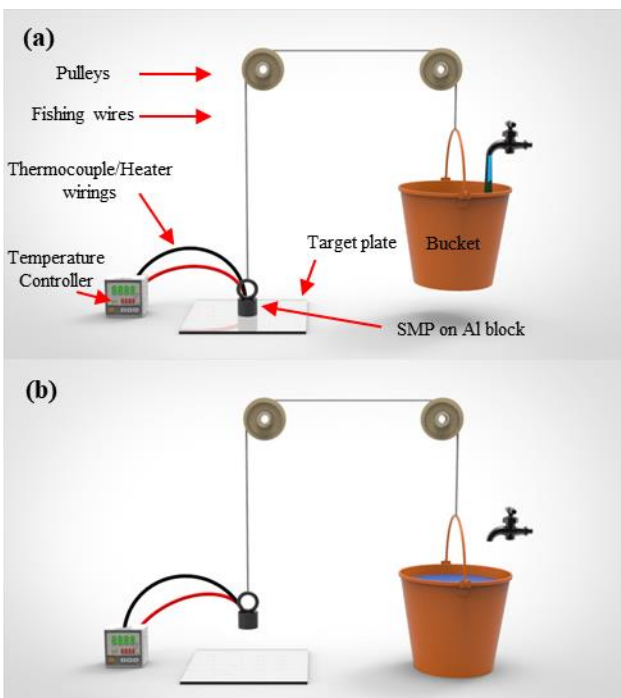

Figure 6 The test setup analyzing the maximum load and the release load. (a) While SMP is attached to the target plate, the bucket is filled with water (b) Once the adhesion strength reaches the maximum, the SMP fails and the bucket falls.

2.5 Heating and Cooling Modules

Fig. 7 shows the two different methods to heat the SMP which commonly involve aluminum plates to separate the SMP from heating sources. The thickness of aluminum plates is chosen to be 2 mm since it is thin enough for heat to reach the SMP but thick enough to have tap holes. When using 22 BNC Nickel-chromium (NiCr) wire as a heating source, 3M 300LSE was used as an insulating pad in order to maximize heat flow toward the SMP. When using a Peltier module (TEC1-12710), a fin was used to release heat such that the whole system does not heat up. Otherwise, the SMP would not be cooled sufficiently. For cooling, natural convection cooling is used when an NiCr wire is used while a Peltier module itself can be used as a cooler by controlling the electrical current direction.

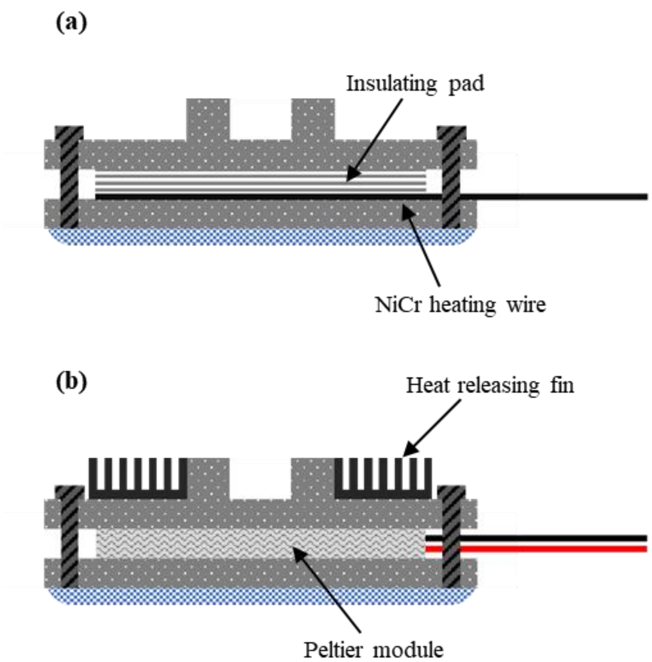

Figure 7 Schematics of the methods to heat SMPs using (a) a NiCr wire and (b) a Peltier module.

CHAPTER 3: RESULTS AND DISCUSSION

3.1 Picking Mechanism

In the pick-up step, the gripper is brought down and the ball joints rotate with appropriate angles to achieve the maximum contact area. Fig. 8a shows the step when applying a preload which is related to the weight of the gripper (F_M) and external force from hand (F_E). Since the preload is critical to adhesive performance [19], it is desirable to have large external force F_E to meet the below inequality where P_{pre} is the minimum preload pressure to ensure reliable adhesive grip.

$$(F_M + F_E) / A > P_{pre} \quad (1)$$

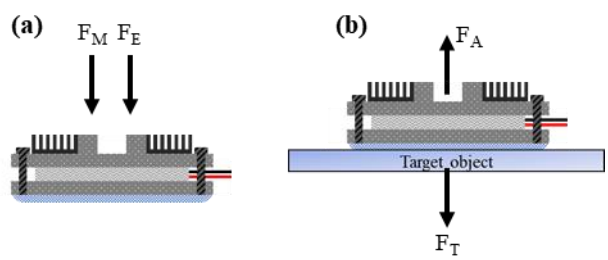

Figure 8 The free body diagram of the foot of an SMP adhesive gripper. Forces during preloading (a) and forces during lifting (b) are shown.

After the SMP achieves its adhesion to the target object, the gripper is able to pick up the target object. In this step, the weight of the target object (F_T) should not exceed the adhesive force of the SMP (F_A) as shown in Fig. 8b. The adhesion strength of the SMP to a flat and smooth glass plate (P_S) is 5-30 N/cm^2, which was characterized elsewhere [20]. Therefore, the maximum weight that the gripper can pick up should be,

$$F_T < F_A = P_S \times A \quad (2)$$

Using the parameters in Table I, F_T should be smaller than 240 N if P_S is assumed to be 5 N/cm^2 and F_T should be smaller than 1440 N if P_S is assumed to be 30 N/cm^2.

Parameter	**Symbol**	**Value**
Weight of the device	F_M	12.7 N
Weight of the target object	F_T	23.5 N
Minimum preload pressure	P_{pre}	15 N/cm^2 [19]
Total SMP area	A	48 cm^2
Angle between the middle link and the leg	θ	0-33.6°
Length from pivot point O to top link	L_a	25 mm
Length from pivot point O to bottom link	L_b	50 mm
Release ring pulling force	F_H	60 N [23]

Table I Parameters of a SMP reversible adhesive gripper

3.2 Placing Mechanism

Fig. 9 shows the two key kinematic mechanisms used in the gripper. One is a ball joint that has a 35° of maximum swivel angle which is used to connect the feet to the gripper legs. Using the ball joints, the gripper can pick up not only flat-surface objects but also curved-surface objects. The other is a pin in slot mechanism with which the middle link is connected to both top link and bottom link. Through this mechanism, a force applied to the releasing ring is converted to the releasing rods with mechanical advantage. Once the SMP adhesive gripper is attached to a target object, the links do not make any displacement such that a static situation can be assumed.

In this static situation, the force is applied from the slot to the pin which is labeled as F_P in Fig. 9b. This force can be split into the horizontal and vertical forces of $F_P \sin\theta$ and $F_P \cos\theta$, and thus

$$F_P = F_P \cos\theta + F_P \sin\theta \tag{3}$$

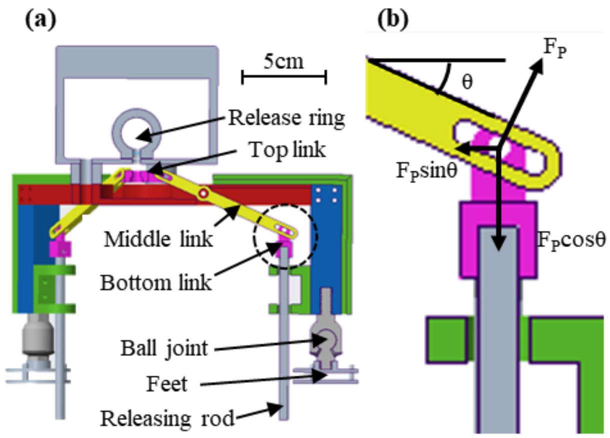

Figure 9 The section view of an SMP adhesive gripper. Pin in slot mechanisms are used between the links.

Evidently, the vertical force ($F_P \cos\theta$) is equal to the reaction force from the ground (F_G) which is labeled in Fig. 10.

$$F_G = F_P \cos\theta \tag{4}$$

In the situation when releasing and placing the target object, having a large F_G is desirable such that the SMP is easily peeled off from the target object. Using (4), F_G can be maximized by setting the initial angle of the middle link θ to be zero.

Fig. 10 shows the forces that are applied to the middle link. F_H is the force that is applied to the release ring per each leg in order to peel off the SMP and place the target object. Simultaneously, reaction force (F_G) is applied from the target object. In a static situation, the sum of the moment at the pivot point O should be zero,

$$\Sigma M_O = F_H L_a - F_G L_b = 0 \tag{5}$$

Where L_a and L_b indicate the distance from point O to the bottom link and the top link. When F_H of 60 N is applied, F_G calculated to be 30 N by using (5) and the parameters in Table I.

Also, for equilibrium of forces, the following equation should be met in a static situation of the middle link in Fig. 10,

$$\Sigma F = F_H + F_G - F_O = 0 \tag{6}$$

Therefore, the force applied to the middle link at point O (F_O) is calculated to be 90 N. Since this force is a force that applied to the middle link, by Newton's third law the leg of the gripper receives the same amount of force as F_O but in opposite direction.

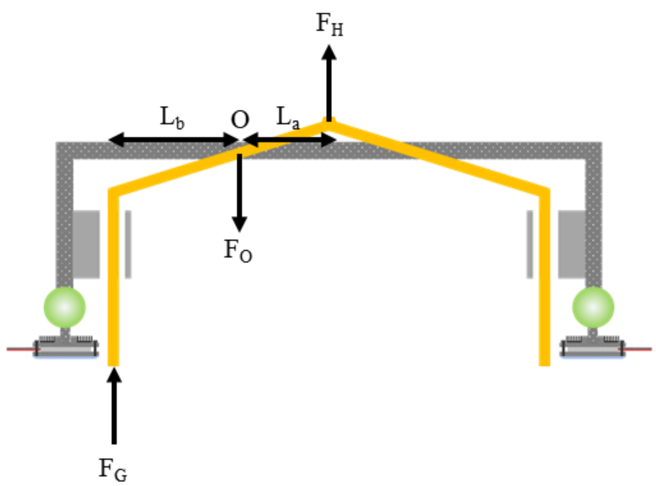

Figure 10 The schematic of an SMP adhesive gripper and its free body diagram of the links.

3.3 Simulation

A finite element analysis(FEA) method on the first principal stress has been conducted to figure out the maximum adhesion strength of single soft or stiff SMP and dual SMP. As shown in Fig. 11(a) the boundary condition is constrained on the SMP bottom which contacts to the target plate. The external load is applied to the top of the aluminum block. Assuming that the SMP is at glassy state at 30 °C, Young's modulus is chosen as 3000 MPa for the stiff SMP and 1500 MPa for the soft. The resultant first principal stress that is applied to the bottom surface of the SMP along the A-A` line is shown in Fig. 11(b). Both stiff and soft single SMP shows extreme high stress concentration at the edge of the SMP. Whereas Dual SMP shows that the stress is more distributed to the center which helps reduce the outer edge stress concentration. As a result of stress distribution from the outer edge to inner center, the crack initialization on the outer edge will start at higher external load for the dual SMP which makes the maximum adhesion strength larger.

Another stress analysis is done by the FEA method to compare the peeling strength of the SMP with and without the release tip. The boundary condition, shown in Fig. 12(a), includes a contact on the bottom surface of SMP and the target plate. Also, a prescribed displacement of 0.74 mm downwards to the target plate has been applied. This value is chosen since the tip height is 0.64 mm and also ensure a small amount of additional compression of 0.1 mm to the rest of the SMP. Assuming that the SMP is at rubbery state at 80 °C, Young's modulus is chosen as 20 MPa. The resultant principal stress that occurs at the bottom surface of SMP along the B-B` line is shown in Fig. 12(b). The SMP without the release tip only shows the compressive stress which increases towards the center. On the other hand, the SMP with the release tip shows dramatical stress concentration and shows both tensile and compressive stress. Consequently, if the prescribed displacement is removed, the SMP with the tip will show easy peeling due to the high concentration of stress near the release tip. Whereas the adhesion strength should be similar since the glassy state SMP after the compression has a similar final contact area on both SMP with or without the release tip.

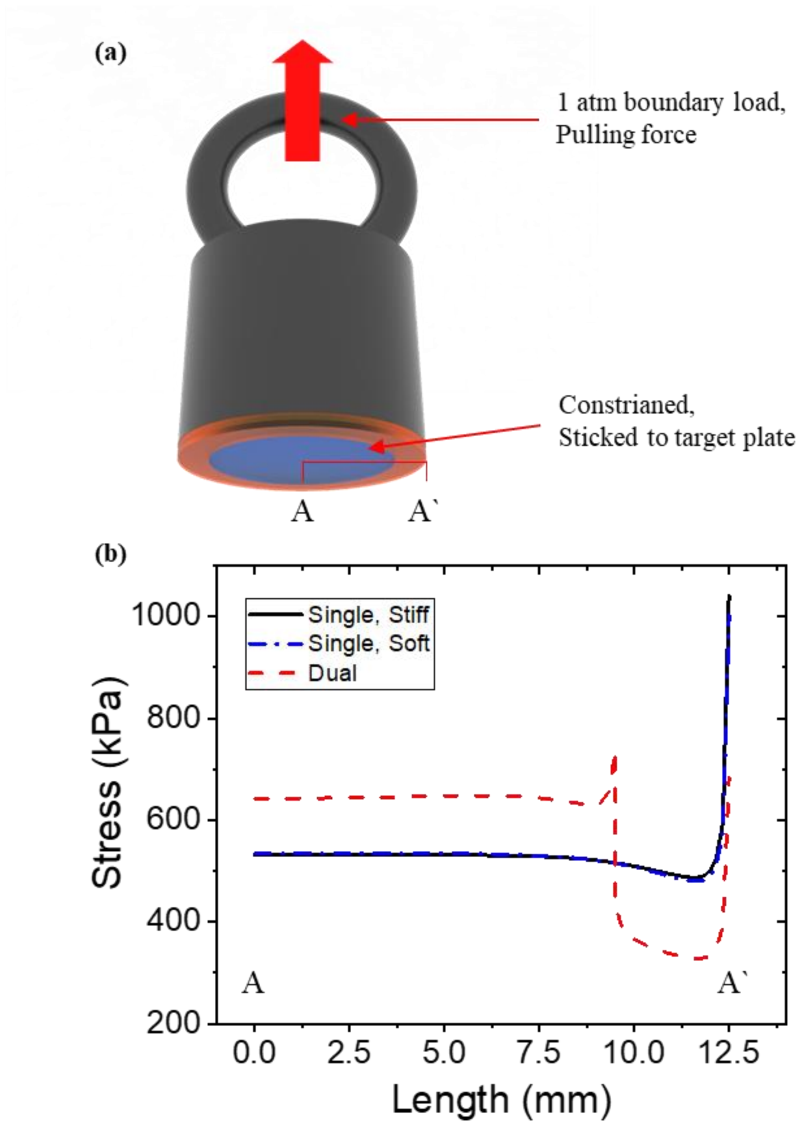

Figure 11 The FEA is conducted on the single SMP and dual SMP along the A-A` line. (a) The schematic of the dual SMP sample attached to the aluminum block and its boundary condition is introduced. (b) The simulation result of FEA along the A-A` line.

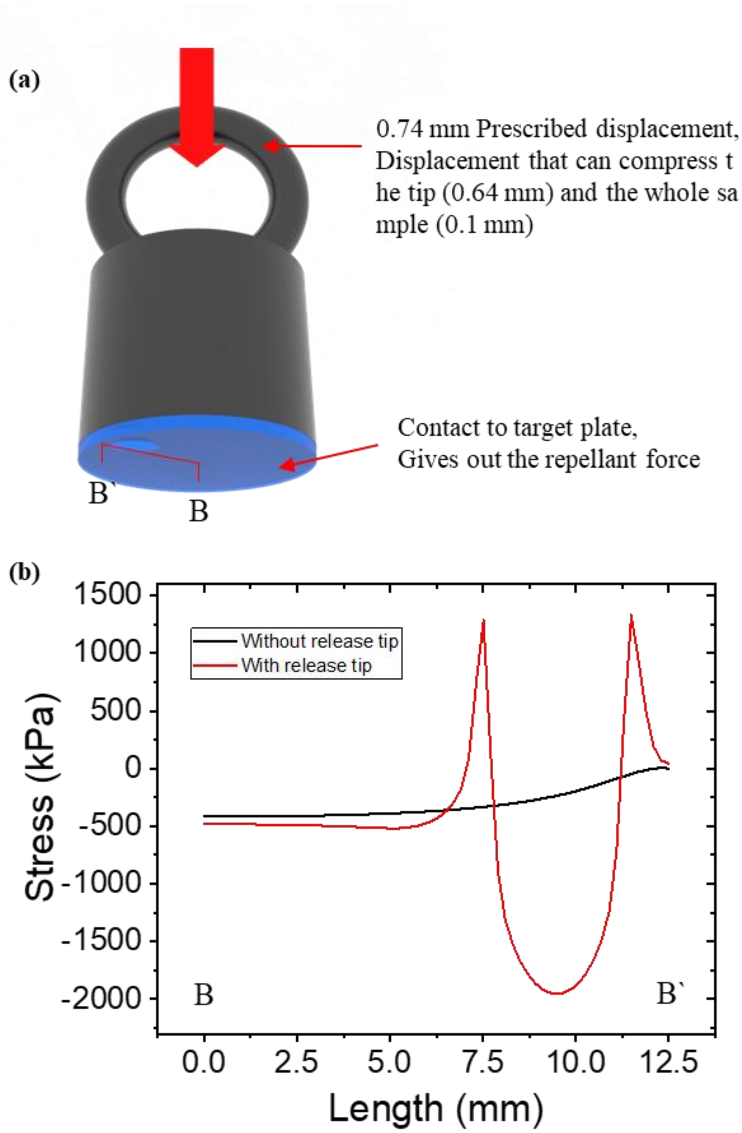

Figure 12 The FEA is conducted on the SMP with and without the release tip along the B-B` line. (a) The schematic of the SMP with the release tip attached to the aluminum block and its boundary condition is introduced. (b) The simulation result of FEA along the B-B` line.

3.4 Experimental results

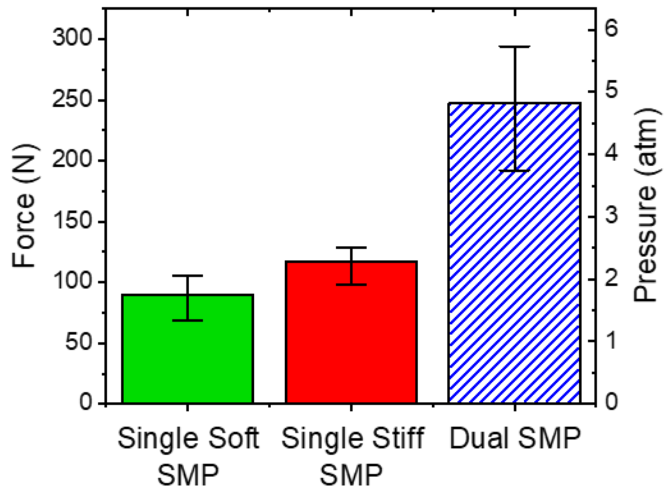

Figure 13 The experimental result of the maximum adhesion strength of the single SMP and the dual SMP.

Fig. 13 shows the result of the maximum adhesion strength using the test setup introduced in Fig. 6. The average adhesion strength for each single soft SMP, single stiff SMP and dual SMP is 1.75 atm, 2.28 atm, 4.83 atm respectively. Fig. 11 shows that the stress concentration for the single soft SMP and the single stiff SMP are almost identical. However, the soft SMP accumulates more strain energy than the stiff SMP and therefore the experimental result of the maximum adhesion strength showed smaller value than the stiff SMP. More importantly, the maximum adhesion strength of the dual SMP came out to be 2.12 times stronger than the single SMP. Usually, the edge of the SMP is more vulnerable to crack initialization. However, as proved in the simulation, the dual SMP distributes the stress from edge to center, and therefore the maximum adhesion strength was considerably higher than the single SMP.

Fig. 14 shows the results of the minimum peeling strength using the test setup introduced in Fig. 6. While the maximum adhesion strength of the SMP with and without the release tip which is the strength upon its failure at the glassy state shows to be 2.35 atm and 1.54 atm respectively. The minimum peeling strength which is the required force to peel off the SMP at the rubbery state is 0.936 atm for SMP without the release tip and 0.00955 atm for the SMP with the release tip. Since the force of the peeling of the SMP with the release tip at the rubbery state is almost negligible, it can be regarded as a self-peeling. The advantage of the self-peeling would be beneficial in a real-life application even though the release tip sacrifices 34 % of the maximum adhesion strength.

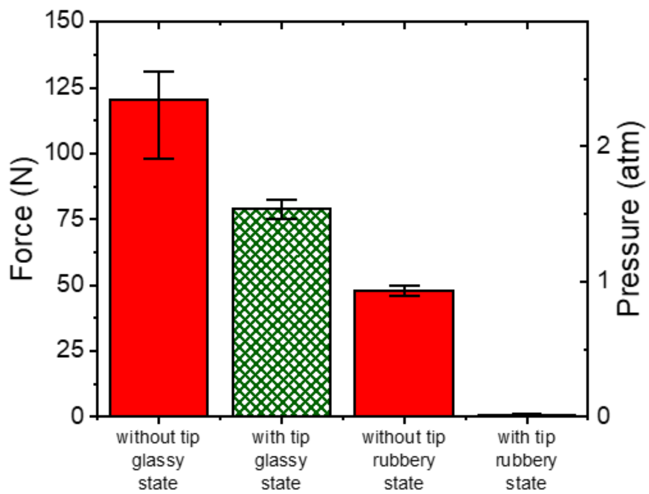

Figure 14 The experimental result of the maximum adhesion strength at the glassy state and the minimum peeling strength at the rubbery state of the SMP with and without the release tip.

3.5 Temperature Analysis

The current SMP mixture has a glass transition at 40 °C. The SMP can act as an adhesive when it is heated, preloaded, and then cooled down below or near T_g. To get the maximum adhesive force, it is desirable to make the SMP rubbery enough by heating it over 80°C and maintaining few seconds for heat to spread out all over the areas of the SMP. Also, fast cooling would help to reduce the chance to be exposed to the external disturbance such as a vibration from human-sourced preload during the rubbery state. For the smooth and easy peeling of the SMP, it is encouraged to raise the temperature up to over 80 °C and maintain to spread the heat out similarly to the adhesion step.

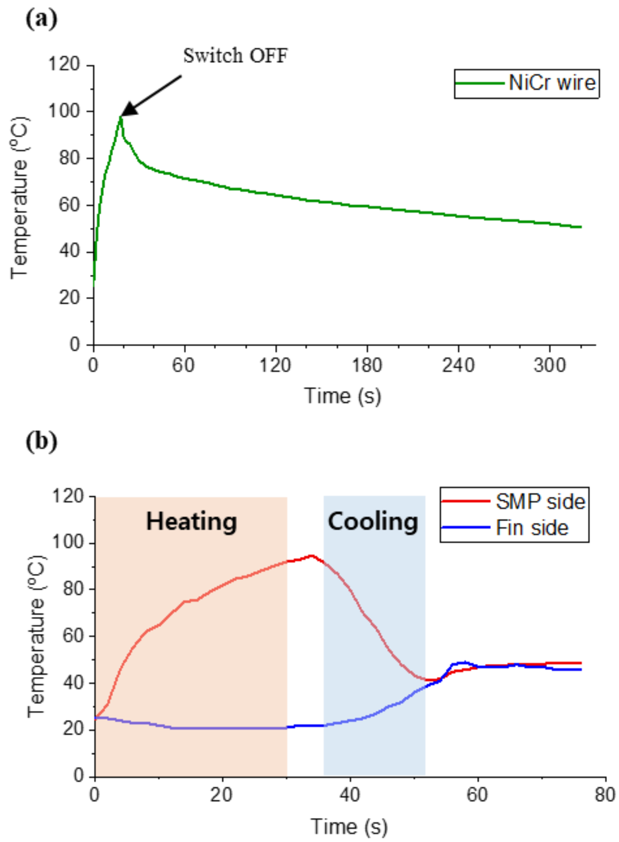

Figure 15 The profile of the temperature as a function of time while using (a) a NiCr heating wire and (b) a Peltier module.

A thermocouple is utilized to characterize the temperature profile of one gripper foot that uses a NiCr wire as a heater sourced by fully charged 3 cell LiPo battery, as Fig. 15a shows. When the switch is turned on, the SMP gets heated. After 15 sec of heating, the SMP reaches 80 °C. At 18 sec, the switch is turned off and the SMP gets cooled. Cooling is done through heat conduction to the whole gripper body and heat convection to the air. At 320 sec, the SMP's temperature finally reaches 50 °C.

Fig. 15b shows the temperature profile of the same gripper foot with a Peltier module operating for both heating and cooling also sourced by fully charged 3 cell LiPo battery. The SMP side indicates the temperature of the SMP and the Fin side indicates the temperature of the heat releasing fin. The first 30 sec of the profile shows that heat flows from the fin side to the

SMP side since the heating switch is on. After 20 sec of heating, the SMP temperature is raised over 80 °C. Between 36 sec and 52 sec the cooling switch is on so that the current flows in the opposite direction. In this condition, the heat flows from the SMP side to fin side which remarkably reduce the cooling time. Immediately after the cooling switch is off, the SMP side temperature becomes about 40 °C. However, since there exists residue heat from the fin side, the final temperature of the SMP side is raised up again to 48 °C and slowly decreases. It is worthwhile to note that high adhesion of the SMP is still achieved even slight above T_g like 40-50 °C since the SMP actually passes through a glass transition temperature range, not a sharp transition at T_g, which can be inferred from Fig.1a.

CHAPTER 4: DEMONSTRATION

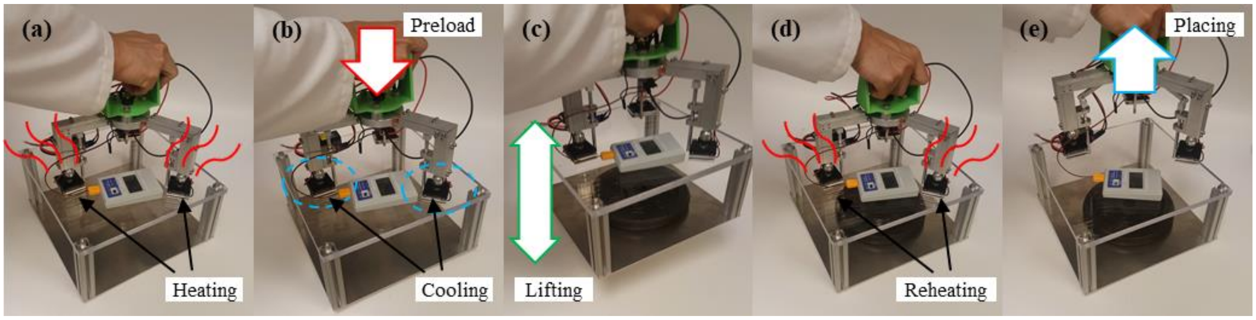

Figure 16 The actual demonstration of an SMP adhesive gripper. The procedure of the pick-and-place demonstration follows: (a) heating the SMP, (b) applying preload and cooling the SMP, (c) lifting the target object, (d) reheating the SMP and (e) separation of the SMP and the target object.

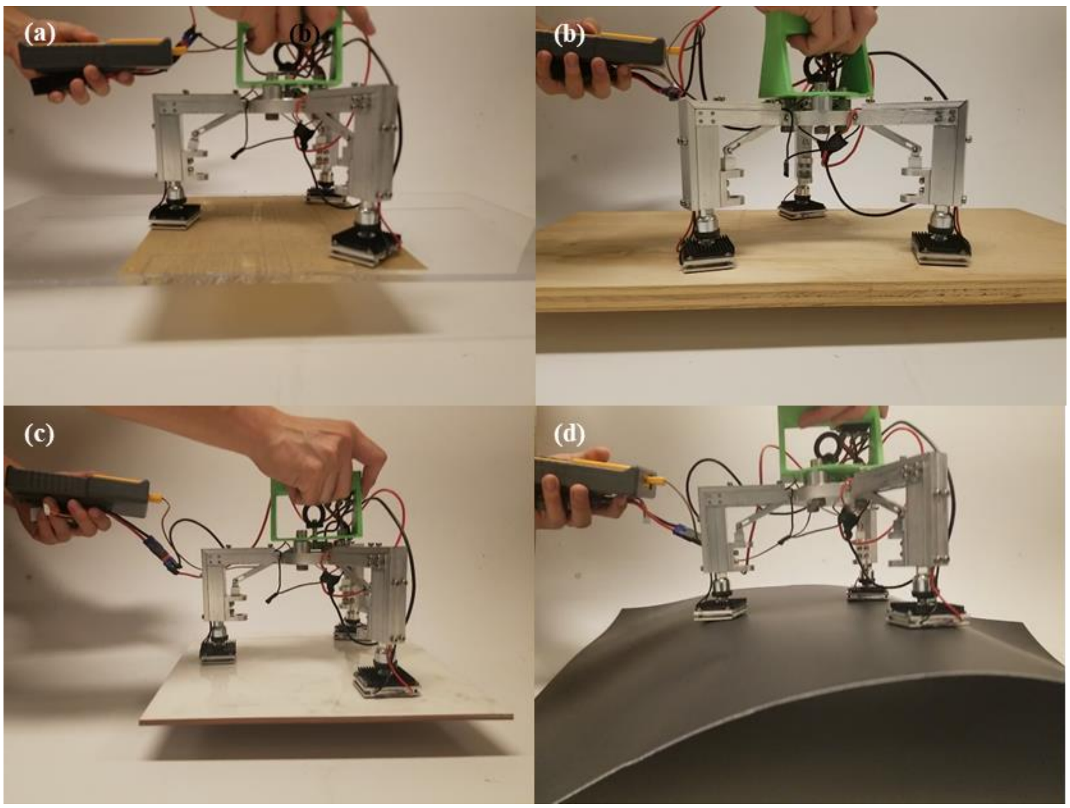

Figure 17 The picking demonstration on various surfaces such as (a) sandpaper, (b) wooden plate, (c) tile, and (d) poster paper are shown.

The presented SMP adhesive gripper is suitable for handling heavy objects with only one hand. Here, a 30 cm × 30 cm × 14 cm stage with an acrylic plastic top is built for the pick-and-place demonstration. Fig. 16a-b show the picking step where the SMP is heated over 90 °C, then preloaded and at the same time cooled down to 40 °C. A mass of 4.5 kg has been added to the stage and the gripper's lifting this weight is tested as shown in Fig. 16c. Finally, Fig. 16d-e show that the SMP is reheated over 90 °C to place the weight.

The SMP is not only capable with smooth flat surfaces such as an acrylic sheet. Fig. 17 demonstrates the SMP adhesive gripper picking up the surface with various roughness and an angled surface. Once the rubbery state SMP perfectly achieves the conformal contact with the target plate and cools down to the glassy state avoiding vibration, it shows the adhesion. This result shows a good prospect on the use of SMP in a practical situation. In addition, Fig. 18 shows that the SMP adhesive gripper is also capable of picking and placing an angled target with 165 and 150 degrees.

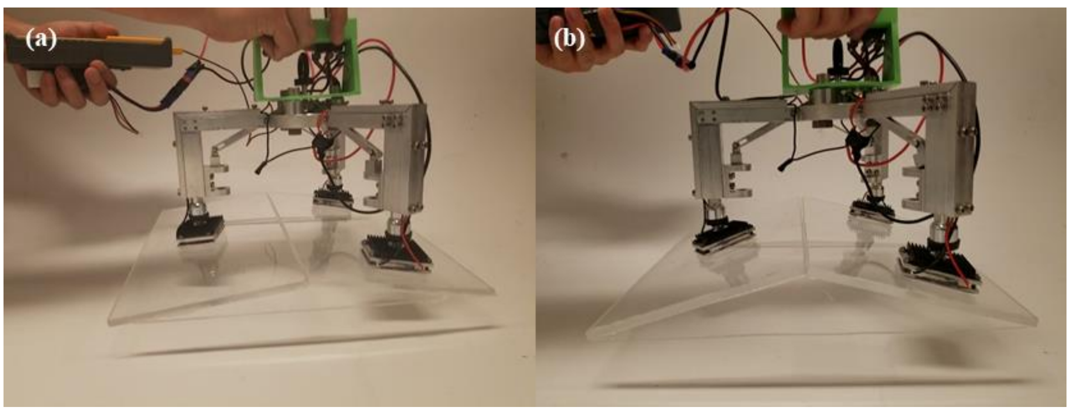

Figure 18 The picking demonstration on angled surfaces of (a) 165 degrees and (b) 150 degrees are shown.

The optical images taken with Keyence VK-X1000 3D laser scanning confocal microscope is shown in Fig. 19. The surface profile of each (a) sandpaper, (b) wood, (c) tile, (d) poster paper and (e) acrylic plate is drawn in an identical scale in Fig. 20. Based on the surface profile, the arithmetic average roughness R_a is calculated for each surface which values are (a) sandpaper 14.1 µm, (b) wood 6.58 µm, (c) tile 0.267 µm, (d) poster paper 2.04 µm and (e) acrylic plate 0.983 µm.

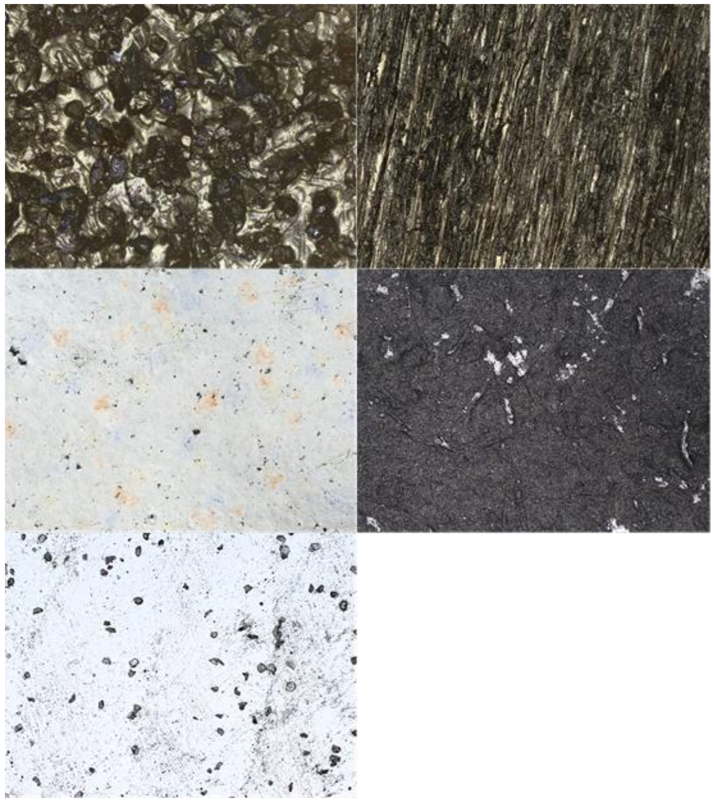

Figure 19 The optical images of (a) sandpaper, (b) wood, (c) tile, (d) poster paper, (e) acrylic plate.

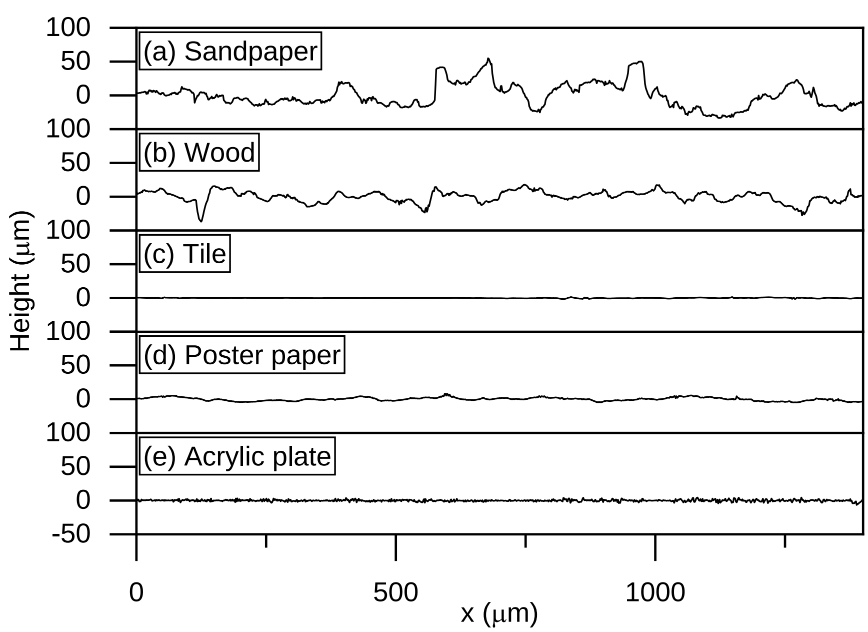

Figure 20 The Surface roughness profiles of (a) sandpaper, (b) wood, (c) tile, (d) poster paper, (e) acrylic plate.

CHAPTER 5: CONCLUSION

In this work, an adhesive gripper utilizing an SMP reversible dry adhesive is designed and tested. First, picking and placing mechanisms are analyzed in particular to enable operating the gripper with a single hand. Since the dual SMP that was fabricated using two different SMP mixture ratios had stress evenly distributed within the whole SMP in the simulation, the adhesin strength was 2.12 times stronger than the single SMP. Also, the SMP with the release tip showed an easy detachment in the experiment and the reason was proved in the simulation that the stress concentration around the tip circumference was considerably high. For heating and cooling, a NiCr wire and a Peltier module are evaluated. Although the Peltier module needs longer time to heat the SMP, the significantly less time for cooling makes it better selection to use since faster cooling allows the SMP adhesion less sensitive to the disturbance of vibration during cooling. The results show the successful pick-and-place capabilities of the SMP adhesive gripper and subsequently the feasibility of the potential use of it for wall climbing applications. For the future work, more quantitative study of the relations between preload and failure, operation angle and failure, and SMP temperature and releasing force will be conducted.

REFERENCES

[1] A. Parness et al., "Gravity-independent Rock-climbing Robot and a Sample Acquisition Tool with Microspine Grippers," *J. of Field Robot.*, vol. 30, no. 6, pp. 897-915, Aug. 2013.

[2] S. Ruggeri, G. Fontana, V. Basile, M. Valori and I. Fassi, "Micro-robotic Handling Solutions for PCB (re-)Manufacturing," Procedia Manuf., vol. 11, pp. 441-448, Jun. 2017.

[3] T. Stoyanov et al., "No More Heavy Lifting: Robotic Solutions to the Container Unloading Problem," *IEEE Robot. Autom. Mag.*, vol. 23, no. 4, pp. 94-106, Aug. 2016.

[4] A. Lourenço, F. Marques, R. Mendonça, E. Pinto and J. Barata, "On the design of the ROBO-PARTNER Intra-factory Logistics Autonomous Robot," in *IEEE Int. Conf. on Syst., Man, Cybern.*, Budapest, 2018., pp. 2647-2652.

[5] C. Feng, Y. Xiao, A. Willette, W. McGee, and V. Kamat, "Towards autonomous robotic in-situ assembly on unstructured construction sites using monocular vision," in *Proc. of the 31th Int. Symp. on Autom. and Robot. in Construction*, 2014, pp. 163-170.

[6] J. Cecil*, D. Vasquez and D. Powell, "A review of gripping and manipulation techniques for micro-assembly applications," *Int. J. of Prod. Res.*, vol. 43, no. 4, pp. 819-828, Feb. 2005.

[7] F. Y. Chen, "Gripping mechanisms for industrial robots," *Mechanism and Mach. Theory*, vol. 17, no. 5, pp. 299-311, Apr. 1982.

[8] K. Telegenov, Y. Tlegenov and A. Shintemirov, "A Low-Cost Open-Source 3-D-Printed Three-Finger Gripper Platform for Research and Educational Purposes," *IEEE Access*, vol. 3, pp. 638-647, May. 2015.

[9] K. H. Cho et al., "A robotic finger driven by twisted and coiled polymer actuator," in *Electroactive Polym. Actuators and Devices (EAPAD) 2016*, Vol. 9798. International Society for Optics and Photonics, 2016, pp. 97981J.

[10] D. Rus and M. T. Tolley, "Design, fabrication and control of soft robots," *Nature*, vol. 521, no. 7553, pp. 467-475, May. 2015.

[11] A. Parness, M. Frost, N. Thatte and J. P. King, "Gravity-independent mobility and drilling on natural rock using microspines," in *Robot. and Autom. (ICRA), 2012 IEEE Int. Conf. on*. IEEE, 2012, pp. 3437-3442.

[12] C. Chen and T. Chung, "A novel thermomagnetic gripper," in *Magn. Conf. (INTERMAG), 2015 IEEE*. IEEE, 2015.

[13] H. Zhang, J. Zhang, G. Zong, W. Wang and R. Liu, "Sky cleaner 3: A real pneumatic climbing robot for glass-wall cleaning," in *IEEE Robot. Autom. Mag.*, 2006, vol. 13, no. 1, pp. 32-41.

[14] T. Miyake, H. Ishihara and T. Tomino, "Vacuum-based wet adhesion system for wall climbing robots-lubricating action and seal action by the liquid." in *Robot. and Biomimetics, 2008. ROBIO 2008. IEEE International Conference on.* IEEE, 2009, pp. 1824-1829.

[15] H. Jiang et al., "A robotic device using gecko-inspired adhesives can grasp and manipulate large objects in microgravity." *Sci. Robot.*, vol. 2, no. 7, Jun. 2017.

[16] S. Song, C. Majidi and M. Sitti, "Geckogripper: A soft, inflatable robotic gripper using gecko-inspired elastomer micro-fiber adhesives," in *Intelligent Robots and Systems (IROS 2014), 2014 IEEE/RSJ International Conference on.* IEEE, 2014. pp. 4624-4629.

[17] J. Shintake, S. Rosset, B. Schubert, D. Floreano and H. Shea, "Versatile Soft Grippers with Intrinsic Electroadhesion Based on Multifunctional Polymer Actuators", *Adv. Mater.*, vol. 28, no. 2, pp. 231-238, 2016.

[18] J. Eisenhaure and S. Kim, "High-strain shape memory polymers as practical dry adhesives," *Int. J. of Adhesion and Adhesives*, vol. 81, pp. 74-78, Mar. 2018.

[19] J. D. Eisenhaure et al., "The use of shape memory polymers for MEMS assembly," *J. of Microelectromechanical Syst.*, vol. 25, no. 1, pp. 69-77, Feb. 2016.

[20] J. Eisenhaure and S. Kim, "An internally heated shape memory polymer dry adhesive," *Polymers*, vol. 6, no. 8, pp. 2274-2286, Aug. 2014.

[21] J. D. Eisenhaure, T. Xie, S. Varghese and S. Kim, "Microstructured shape memory polymer surfaces with reversible dry adhesion," *ACS applied materials & interfaces*, vol. 5, no. 16, pp. 7714–7717, Aug. 2013.

[22] M. D. Bartlett et al., “Looking beyond fibrillar features to scale gecko-like adhesion,” *Adv. Mater.*, vol. 24, no. 8, pp. 1078-1083, Jan. 2012.

[23] A. D. Astin, “Finger force capability: measurement and prediction using anthropometric and myoelectric measures,” M.S. thesis, Dept. Ind. and Syst. Eng., Virginia Tech, Blacksburg, VA, 1999.